Acta Mechanica Slovaca **27 (1): 40 - 47,** March **2023**
https://doi.org/10.21496/ams.2023.019

Acta Mechanica Slovaca
ISSN 1335-2393
www.actamechanica.sk

Numerical Modelling of Flow in Fluidic Oscillator

Tomáš Blejchař [1,*], Sylva Drábková [1], Václav Janus [2]

[1] VSB -Technical University of Ostrava, Faculty of Mechanical Engineering, 17. listopadu 2172/15, 70800 Ostrava
[2] VSB -Technical University of Ostrava, Faculty of Electrical Engineering, 17. listopadu 2172/15, 70800 Ostrava

Abstract: The systems with fluidic oscillators are intensively studied nowadays because the oscillatory flow can increase heat and mass transfer and decrease energy dissipation. Fluidic oscillators produce an active-type mixing enhancement but in a passive manner as they do not require any moving parts. They convert steady pressurized inlet flow to oscillatory or pulsatile flow at an outlet without the need for external power. In general, there are many types of fluidic oscillators, categorized by the underlying mechanism to create oscillatory output behaviour. The fluidic oscillator with the single feedback loop is analysed in this paper. A numerical simulation of oscillating flow is performed and two approaches for modelling flow, RANS, and LES are applied especially. The results of numerical simulation are compared with experimental measurement. The analysis is focused on pressure drop and oscillation frequency dependent on the inlet conditions. The energy spectrum of oscillating flow is analysed using discrete Fourier transform.

Keywords: fluidic oscillator; single feedback loop; oscillation frequency; numerical modelling; measurement.

1. Introduction

Fluidic oscillators are relatively simple devices with generally no moving parts. Their design goes back to the 60 s and 70 s when the first fluidic flow meters were invented, patented [1] and applied [2]. Since that time, the range of their application has increased significantly. They are used as actuators for the flow control [1], [3], in combustion control [4], boundary layer modification in turbomachinery [5], flow separation control on aerofoils [6], noise reduction in cavities [7] and many other fields. Growing interest in their application has brought the need for better understanding of the internal flow patterns and the oscillation mechanism. The first analyses were carried out experimentally, e.g. [8]. Later, numerical investigations of fluidic oscillators were performed to understand the unsteady internal flow field and geometrical effects on its performance [9], [10].

The fluidic oscillator usually consists of one supply port, two output ports and two control ports along with their feedback loop. There are two main designs of fluidic flowmeters working on different principles, illustrated in Fig.1 [2]. The first (a) is designed with one feedback loop, the second (b) features two feedback channels. The fluidic oscillator with the single feedback loop is mainly governed by the physical phenomenon known as the Coanda effect, which attaches fluid stream alternatively to one of adjacent walls in the mixing chamber. The geometric shape of the Coanda flowmeters generates a continuous, self-induced oscillation. Due to this switching characteristic, they are considered as a pressure driven devices. The frequency of the jet's oscillation is a function of the oscillator's design, size, and supply rate.

Since the structures of different fluidic oscillators and their flow dynamics differ, their affecting parameters are also different and are subjected to studies and investigation. The objective of this paper was to investigate the performance of the Coanda fluidic

*** Corresponding author:** Tomáš Blejchař, ***E-mail address:*** *tomas.blejchar@vsb.cz*

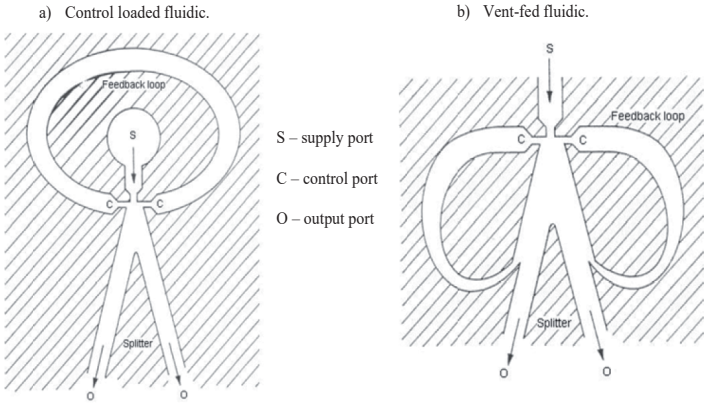

Figure 1: Standard designs of fluidic oscillators [2].

oscillator presented in the recent study [11] by McDonough, Law, Kraemer, and Harvey. The authors focused on experimental analysing the effects of varying fluidic oscillator geometries on the flow-switching frequencies as well as the effect of working liquid physical properties. The outcomes of their work inspired us to carry out numerical analysis. The current paper presents a numerical simulation of the basic fluidic oscillator configuration presented in [11] and illustrated in Fig.2. The fluidic device operated with water was tested numerically via 3D computational fluid dynamics (CFD). The performance was evaluated at low Reynolds numbers and compared with the experimental measurement. The main objective was to understand the unsteady internal flow field connected with the switching mechanism of the fluidic oscillator and compare the results obtained with RANS and LES turbulence models.

2. Fluidic geometry model

Fig. 2 shows the basic design of the fluidic oscillator [11]. The single feedback loop design includes a supply port, two outlet channels and two control ports that are connected through a single feedback loop. The main geometrical parameters define 1 mm nozzle constriction size and 25 mm nozzle convergence length, with a total inlet distance of 32 mm. A splitter with 1 mm diameter con-cave wall is positioned after the nozzle at a distance of 7 mm. Also located adjacent to the nozzle are two control ports, connected by a 3 mm wide and 101 mm long feedback loop. Due to the position of the feedback loop, the liquid is supplied via a 90°bend, converging from an 8 mm to 4 mm tube diameter. The two outlet channels are 65 mm long and the diameters of the outlet ports are 4 mm.

Fluid jet emerging from a nozzle bends toward and attaches itself to an adjacent surface. A low-pressure vortex forms between the attachment wall and the attached jet. A portion of the flow with higher pressure passes through a feedback loop and travels back to the control port. This feedback flow breaks the jet attachment and pushes it toward the opposite sidewall. The frequency of switching is proportional to the volume flow rate. Flow-switching between two channels results in dual pulsatile flows. These pulsatile flows could be used for process intensification.

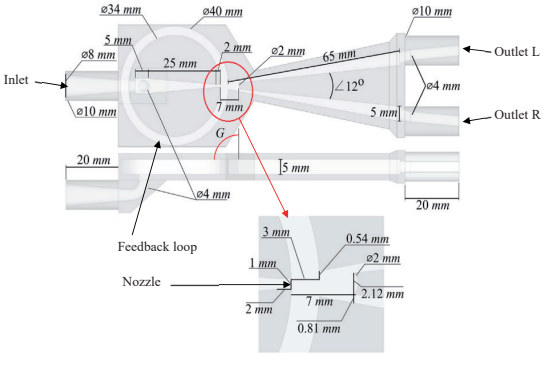

Figure 2: Geometrical design of the fluidic oscillator with single feedback channel [11].

The dimensionless numbers are very useful to characterize flow and its parameters. One of the most important is the Reynolds number,

$$Re = \frac{u \cdot d_h}{\nu} \qquad (1)$$

where d_h is hydraulic diameter of relevant channel, u

is mean velocity and v is kinematic viscosity.

Fluidic oscillators can be characterized by three Reynolds numbers. As the first, it is the inlet Reynolds number, which is related to inlet pipe, and defines inlet flow. Second, the Jet Reynolds number corresponds to nozzle throat and characterizes main flow directly related to the natural frequency of fluidic oscillator. The last one is the Feedback loop Reynolds number, characterizing flow in feedback loop.

Next dimensionless criterion necessary to estimation of parameters is Strouhal number,

$$Sr = \frac{f \cdot d}{u} \qquad (2)$$

where d is characteristic dimension, (often nozzle throat), f is frequency of oscillation and u is velocity, usually average velocity at nozzle throat. Fluidic oscillator usually operates under nearly constant Strouhal number as the frequency response is proportional to the increase in velocity.

3. Experimental measurement

3.1. Fluidic oscillator prototype

Analysis of the fluctuation flow in fluidic oscillator with single feed-back loop was carried out in the laboratory of the Department of Hydromechanics and Hydraulic Equipment. The fluidic oscillator prototype was made by 3D printing. Design for 3D print was made in Fusion360 CAD software considering geometry and dimensions presented in Fig. 2. The whole body of the fluidic was made with PLA and PET-G on a Prusa mk3 printer. The G1/4 threads were prepared for the connection of the pressure transducers at inlet and both outlets. Two piezo-resistive pressure sensors with integrated A/D converter and signal processor were used to measure the pressure drop on fluidic oscillator Δp and pressure 1 (upstream) and pressure 2 (downstream) respectively. The sensors were installed close to the inlet and outlet fitting of fluidic via T-junction. Another two pressure sensors of the same type were used to measure the pressure fluctuation in the left and right channels of the fluidic. Fig. 3 shows the placement of the transducers and fittings around the fluidic oscillator.

3.2. Experimental setup

The experimental setup developed to observe pressure drop of oscillator and pressure fluctuation in outlet channels and a structure is depicted in Fig.4.

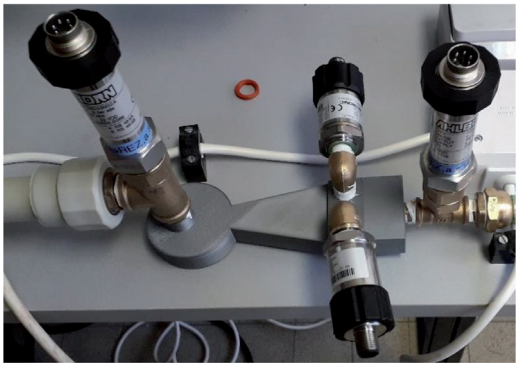

Figure 3: Pressure transducers installed on the fluidic oscillator prototype.

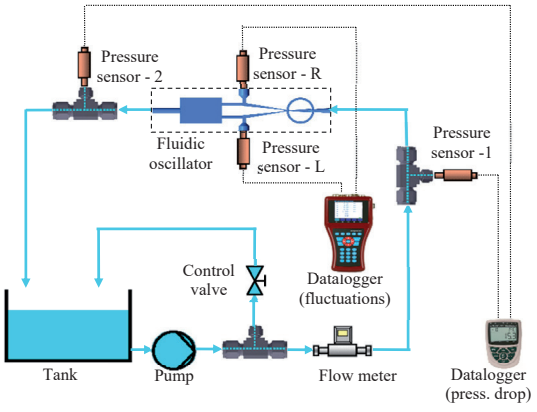

Figure 4: Experimental setup.

The flowing medium was water which was taken from the water supply line in the laboratory. The centrifugal pump was used as a source of hydraulic energy. The flow rate of water through the fluidic was set by the manual by-pass control valve. Volume flow rate was measured using an induction flow meter with range (10-2500) l/h. Measurement was performed for seven flow rates in range 20-130 l/h. The hydraulic circuit was left without manipulation approximately 1 minute to calm the flow and other parameters and eliminate influence of transient phenomenon respectively. Thereafter the measurement was started and 2 minutes time record of volume flow, pressure (Sensor L and R), pressure drop (Sensor 1 and 2) was made. This procedure was repeated for every set volume flow. Upstream and downstream pressure (Sensor 1 and 2) was measured with sampling period Δt = 0.3 s. The „left" and „right" pressure (Sensor L and R) were measured with sampling period Δt = 1 ms.

3.3. Results of Experiment

The results of experimental measurement are

summarized in Table 1. The variable Δp_{Fl} was defined as absolute value of $p_L - p_R$ pressure difference.

$$\Delta p_{Fl} = |p_L - p_R| \quad (3)$$

The discrete Fourier transform (DFT) analysis of periodic pressure fluctuation Δp_{Fl} was used for estimation of frequency f_0 and amplitude p_A of the periodic signal of Δp_{Fl}. According to the Nyquist–Shannon sampling theorem, the maximum measurable frequency of fluctuations was ca 400Hz, which was sufficient in this case, as the expected frequency of fluctuation was below 50 Hz. Type A and Type B uncertainty were evaluated for every measured variable in Tab. 1 (4x pressure, 1x volume flow rate). Strouhal number based on the frequency of generated oscillation, the width of the main (supply) nozzle and bulk velocity in the exit of this nozzle was calculated as well.

Table 1: Summary results of experimental measurement.

Meas. no.	Q [l/h]	$\Delta p=p_1-p_2$ [kPa]	p_A [kPa]	fo [Hz]	Sr_{jet} [-]
1	20±3	2.3±0.5	0.4±0.2	2.92±0.02	0.0044±0.0004
2	30±3	6.6±0.6	0.5±0.2	4.88±0.05	0.0049±0.0003
3	40±3	9.8±0.6	0.6±0.2	6.83±0.09	0.0051±0.0002
4	700±3	22.3±0.7	0.9±0.2	11.72±0.27	0.0050±0.0002
5	90±3	30.5±0.7	1.2±0.2	15.60±0.49	0.0052±0.0002
6	110±3	50.1±0.9	2.0±0.2	21.48±0.92	0.0059±0.0004
7	130±3	71.0±1.2	2.5±0.2	26.36±1.39	0.0061±0.0006

Fig. 5 shows the short time record of pressures pL and pR measured at both outlets of the fluidic oscillator for the flow rate corresponding to the measurement number 7. Pressure fluctuations illustrate the fully turbulent flow inside the fluidic oscillator, the amplitude peaks are chaotic, and the pressure fluctuation signal is not like a smooth function e.g., sinus.

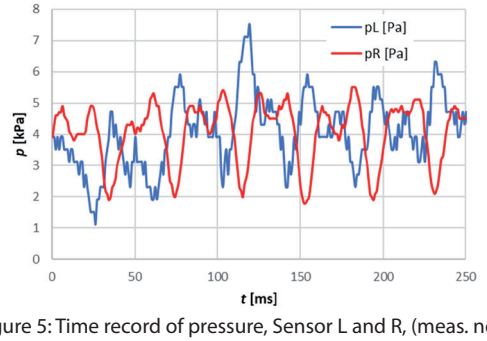

Figure 5: Time record of pressure, Sensor L and R, (meas. no 7).

Fig. 6 shows the pressure fluctuation Δp_{Fl} time history. The time record of Δp_{Fl} was further subjected to DFT analysis to find the dominant frequency, as presented in Fig. 7. The dominant eigenfrequency (i.e. natural frequency) and other frequencies were estimated on the base of the power spectral density. The power spectral density (PSD) refers to the spectral energy distribution per unite time and summation or integration of PSD yields the total power of signal.

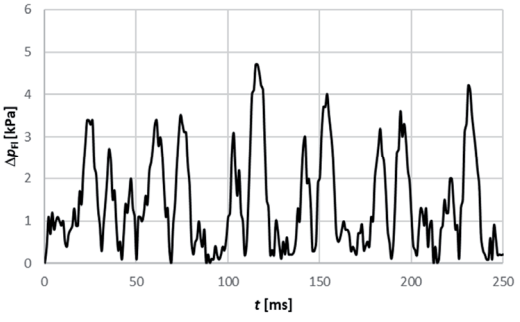

Figure 6: Time record of pressure fluctuations Δp_{Fl}, (meas. no 7).

Fig. 7 shows first and second harmonic corresponding to stable sinusoidal oscillation.

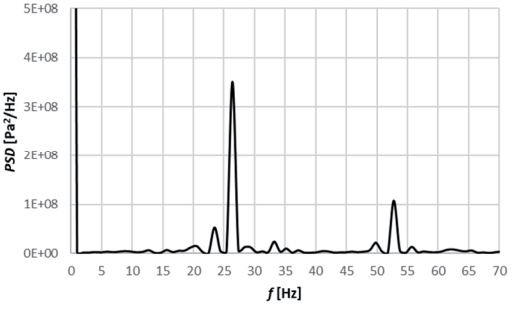

Figure 7: DFT analysis of pressure fluctuation Δp_{Fl}, (meas. no 7).

4. Numerical Simulation

Measurement was followed with the CFD analysis. The flow was considered as turbulent, incompressible due to the low static pressure and low compressibility of water and isothermal in this study. All simulations were 3D and transient which follows from the periodic flow in fluidic. The RANS and LES approach for simulation of unsteady flow was tested. The computational grid was created as pure hexahedral. The grid was generated as one half, then mirrored, and connected in CFD code. This procedure provided symmetric computational

mesh necessary for modelling the periodic flow. The final mesh with ca 5 million cells was used in CFD code after the independent test.

3.1. Governing Equations

The governing equations describing the flow in fluidic oscillator can be found in many CFD textbooks [12] or [13]. Mass and momentum conservation for incompressible and isothermal flow is defined as follows:

$$\frac{\partial u_j}{\partial x_j} = 0 \tag{4}$$

$$\frac{\partial u_i}{\partial t} + \frac{\partial \left(u_i u_j\right)}{\partial x_j} = -\frac{1}{\rho}\frac{\partial p}{\partial x_i} + \nu \frac{\partial^2 u_i}{\partial x_j^{\,2}} \tag{5}$$

where $\vec{u}$, p, ρ, ν are velocity, pressure, density, and kinematic viscosity of the fluid. As the flow was modelled as turbulent, this basic mathematical model was further extended with additional transport equations. Shear stress transport k-ω model was chosen from RANS family due to high shear stress, jet flow, and low Reynolds number in the fluidic oscillator. The second turbulent model was based on LES approach, which solves large turbulent eddies directly and sub grid eddies statistically instead RANS models, which solve all eddies statistically. The LES WALE turbulent model was chosen from LES family, because it can predict near wall turbulence more precisely, which is very important for flow with high velocity gradient. The governing equations were solved by finite volume method employed in CFD software Ansys CFX.

3.2. Results of CFD simulations

The table Tab.2 summarizes results of numerical simulation for both approaches RANS and LES.

Table 2: Summary results of numerical simulation.

no	Q [l/h]	$\Delta p=p_1-p_2$ [kPa]		p_A [kPa]		fo [Hz]		Sr_{jet} [-]	
Approach		RANS	LES	RANS	LES	RANS	LES	RANS	LES
1	16	0.7	0.9	0.1	0.1	2.47	2.83	0.0046	0.0053
2	32	2.6	2.9	0.3	0.3	5.51	6.11	0.0052	0.0057
3	64	9.5	9.7	1.3	1.2	12.35	12.75	0.0058	0.0060
4	128	35.6	35.3	4.4	4.6	26.86	25.88	0.0063	0.0061

Both outlet port channels include plug for installing sensors p_L and p_R. Static pressure was monitored in plugs on surface like sensors membrane. The pressure was recorded as area weighted average. Same as in measurement, the performance of the fluidic oscillator was evaluated using frequency of oscillation f_0, amplitude of pressure fluctuations pA and the pressure drop Δp through the fluidic oscillator. To analyse the frequency response, the discrete Fourier transform (DFT) on each recorded waveform from the pressure transducers was performed.

The velocity flow field is visualized on mid – plane of the fluidic oscillator. The non-stationary flow is illustrated by discrete figures for 0.2; 0.4; 0.6; 0.8 and 1 multiple of the main oscillation period, as can be seen in Fig. 8.

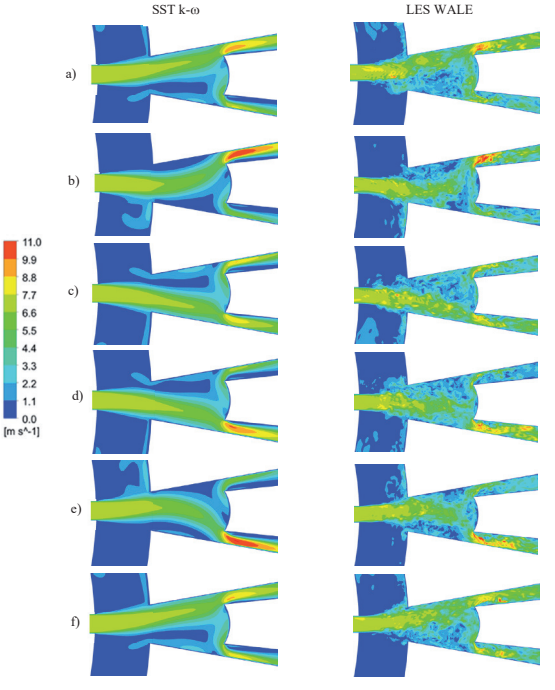

Figure 8: Results of numerical simulation, visualization of velocity field, RANS left column, LES right column, Q=128 l/h, CFD no. 4.

The so-called Coanda effect can be clearly observed, which influences the jet. The generated jet crosses the exit nozzle and encounters the splitter, which divides the flow towards both outlets. This flow configuration is unstable, the jet starts to perform motion in the crossflow direction and collides with the upper wall at the end of the mixing chamber. A part of the flow is directed through the feedback loop pushing the main jet towards the opposite wall, however the jet has tendency to flow

to the same port (see Fig. 8 b and 8e). As a result, the self-sustained jet oscillation dynamics develops.

The difference between RANS and LES approach to turbulence modelling can be clearly observed. The physics is essentially the same for both, but the solved equations are different. RANS can account for dominant coherent structures in the flow, while LES is capable to reveal the eddies hidden behind the mean in RANS. The same computational grid and identical boundary conditions were applied. LES was generally more time consuming when compared with RANS, as longer time was required to establish the regular oscillations.

5. Discussion of Results and Conclusion

The data obtained from numerical simulation and measurement were further compared in following Fig. 9, 10, 11. One of the main characteristics of a fluidic oscillator is linear frequency behaviour versus the inlet flow rate. This comparison is presented in Fig. 9 and clarifies that the expected linear behaviour appears both in numerical and experimental results. RANS and LES models estimates almost identical eigenfrequency of the main flow in the full range of flow rate.

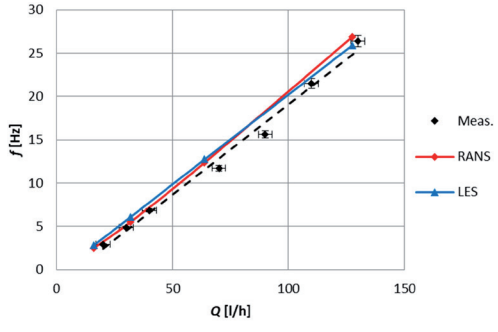

Figure 9: Frequency of oscillation as a function of flow rate, comparison of meas. and CFD.

The dependence of Strouhal number on the flow rate has the comparable trend both in case of measurement and numerical modelling, as can be seen on the Fig. 10. Measurement shows higher values of pressure drop $\Delta p = p_1 - p_2$ than predicted in the numerical simulation. This may be due to the additional losses in junctions, internal roughness in fluidic, etc. that cannot be included into mathematical model, see Fig. 11.

In the opposite, the pressure amplitude p_A of pressure oscillations Δp_{Fl} predicted with numerical simulation, is higher in comparison with

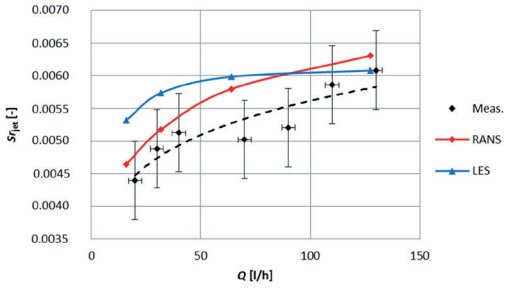

Figure 10: Strouhal number as a function of flow rate, comparison of meas. and CFD.

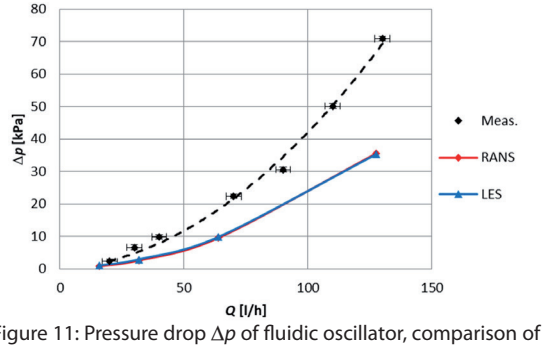

Figure 11: Pressure drop Δp of fluidic oscillator, comparison of meas. and CFD.

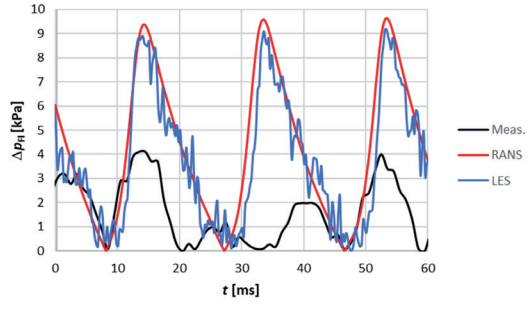

Figure 12: Pressure fluctuation p_{Fl}, comparison of measurement no 7 vs CFD no 4. (Same flow rate).

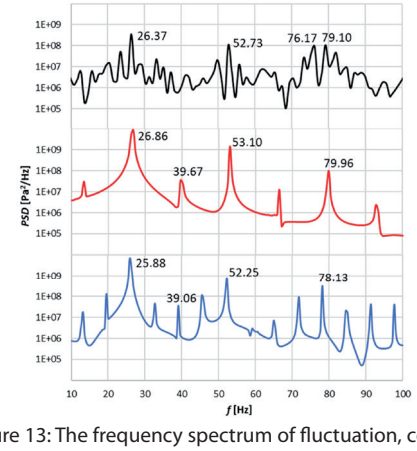

Figure 13: The frequency spectrum of fluctuation, comparison of meas. no 7 vs CFD no 4. (Same flow rate).

measurement see Fig. 12. It can be caused by low sensitivity of sensor L and P or worse dynamic characteristics of sensors. It would be better to use faster and sensitive sensor instead used ones. Measuring of pressure difference Δp_{Fl} directly by pressure difference sensor is another possible variant, which could eliminate parameter differences between two sensors, because they should be absolute same, but it is technically impossible. More than absolute value of pressure fluctuation, the frequency of oscillation was more interesting. Time record of pressure fluctuation was analysed by DFT. The comparison of the frequency spectrum is performed in Fig. 13. It is obvious that both RANS and LES approach is precisely able to predict the main oscillation frequency. The LES approach solves the flow field as chaotic, so the frequency spectrum contains much more frequencies than the RANS approach which is time filtered.

6. Summary

The design of water-operated fluidic oscillator presented in [11] has been investigated using CFD simulations and measurement on the 3D printed prototype. Unsteady RANS and LES simulations of a fluidic oscillator were carried out and the performance was investigated in varying Reynolds numbers. The performance of the fluidic oscillator was evaluated using frequency of oscillation f_0, amplitude of pressure fluctuations Δp_{Fl} and the pressure drop Δp through the fluidic oscillator. Linear relationship between the frequency of oscillation and flow rate was reached both in numerical simulation and measurement, as expected from several other studies on fluidic oscillators [3], [4]. Frequencies of 2–27 Hz were produced for kinematic viscosities of 1.10^{-6} m^2/s, in the range of Q = 20-130 l/h. Pressure loss measured on the prototype was higher than that predicted by the numerical modelling. The frequency of oscillation predicted by CFD is equal to the measured one, the first, and second harmonic frequency especially. As a result, three-dimensional simulations provided good estimations of the operating frequency of the fluidic oscillator when compared with experimental measurements in a range of Reynolds numbers. Numerical analysis is capable to investigate the complexity of the turbulent flow dynamics inside the fluidic oscillator. It can be used as a tool for evaluating the effect of designed geometric modifications and prediction of fluidic device performance in specific applications.

However, there are many questions left in connection with this topic, so further investigation of flow in fluid oscillation is expected and recommended. Future work will focus on improvement of the experimental setup, mainly the measurement technique. Sensors with better dynamic characteristics and higher sensitivity are necessary for measuring of pressure pulsations and improving the validity of experiment.

Acknowledgments

Main text paragraph This work has received funding from the European Union's Horizon 2020 research and innovation programme under grant agreement no. 856670; the developing was funded by the project CZ.01.1.02/0.0/0.0/15_019/0004955 "Energy Harvesting from environment free of Battery Supply to Measuring energy consumption in the SMART Grid Network" of the Operational Program of Business and Innovation for Competitiveness.

References and Notes

1. Woszidlo, R., et al. Fundamental properties of fluidic oscillators for flow control applications. AIAA J. 2019, 57, pp. 978–992.
2. Morris, N. M., 'An Introduction to Fluid Logic', McGraw-Hill, 1973
3. Gregory, J. W. and Tomac, M. N. A review of fluidic oscillator development and application for flow control, AIAA Paper, 2013, 2474.
4. Guyot, D., et al. Active combustion control using a fluidic oscillator for asymmetric fuel flow modulation. In Proceedings of the 44th AIAA/ASME/SAE/ASEE Joint Propulsion Conference & Exhibit, Hartford, CT, USA, 21–23 July 2008; p. 4956
5. Cerretelli, C. and Kirtley, K. Boundary layer separation control with fluidic oscillators. J. Turbomach. 2009, 131, 041001.
6. Tesař, V. Pressure -Driven Microfluidic. Artech House Publishers, Norwood, USA. 2007. ISBN-10:1596931345
7. Raman, G. and Raghu, S. Cavity resonance suppression using miniature fluidic oscillators, AIAA Paper (2012) pp. 2608-2612.
8. Bobusch, B. C., et al. Experimental study of the internal flow structures inside a fluidic oscillator. Exp. Fluids 2013, 54, p. 1559.
9. Krüger, O., et al. Numerical Modeling and Validation of the Flow in a Fluidic Oscillator. In Proceedings of the 21st AIAA Computational Fluid Dynamics Conference, San Diego, CA, USA, 24–27 June 2013; p. 3087.
10. Pandey, R. J. and Kim, K. Y. Numerical modeling of internal

flow in a fluidic oscillator. J. Mech. Sci. Technol. 2018, 32, pp. 1041–1048.

11. McDonough, J. R., et al. Effect of geometrical parameters on flow-switching frequencies in 3D printed fluidic oscillators containing different liquids. J. chemical engineering research and design 117, 2017, pp. 228–239

12. Anderson Jr., J. D. Computational Fluid Dynamics. The Basics with Applications, McGraw-Hill, USA, 1995. ISBN 0-07-001685-2

13. Ferziger, J. H. and Peric, M. Computational methods for fluid dynamics. Berlin: Springer, 1996. ISBN 3-540-59434-5